Published OnlineFirst February 28, 2010; DOI: 10.1158/0008-5472.CAN-09-2833

Cancer Research

Talin1 Promotes Tumor Invasion and Metastasis via Focal Adhesion Signaling and Anoikis Resistance

Shinichi Sakamoto[1], Richard O. McCann[2], Rajiv Dhir[3], and Natasha Kyprianou[1,4,5]

Abstract

Talin1 is a focal adhesion complex protein that regulates integrin interactions with ECM. This study investigated the significance of talin1 in prostate cancer progression to metastasis *in vitro* and *in vivo*. Talin1 overexpression enhanced prostate cancer cell adhesion, migration, and invasion by activating survival signals and conferring resistance to anoikis. ShRNA-mediated talin1 loss led to a significant suppression of prostate cancer cell migration and transendothelial invasion *in vitro* and a significant inhibition of prostate cancer metastasis *in vivo*. Talin1-regulated cell survival signals via phosphorylation of focal adhesion complex proteins, such as focal adhesion kinase and Src, and downstream activation of AKT. Targeting AKT activation led to a significant reduction of talin1-mediated prostate cancer cell invasion. Furthermore, talin1 immunoreactivity directly correlated with prostate tumor progression to metastasis in the transgenic adenocarcinoma mouse prostate mouse model. Talin1 profiling in human prostate specimens revealed a significantly higher expression of cytoplasmic talin1 in metastatic tissue compared with primary prostate tumors ($P < 0.0001$). These findings suggest (*a*) a therapeutic significance of disrupting talin1 signaling/focal adhesion interactions in targeting metastatic prostate cancer and (*b*) a potential value for talin1 as a marker of tumor progression to metastasis.

Cancer Res; 70(5); 1885–95. ©2010 AACR.

Introduction

Cancer metastasis is a multistep and complex process that involves dissociation of the tumor cells from the organ of origin, degradation of the ECM, cell migration, anchorage-independent growth, apoptosis evasion, angiogenesis, invasion of surrounding tissues, cell adhesion, movement, and colonization to distant sites in the body (1). Human prostate cancer progression to advanced metastatic disease is associated with relapse to a hormone refractory state due to impaired apoptotic response to androgen ablation. Androgen-independent prostate cancer cells become resistant due to roadblocks in apoptosis and, depending on the interactions with the tumor microenvironment, acquire invasive and metastatic properties (2). Both tumor epithelial and endothelial cells require attachment to the ECM for survival, and upon loss of adhesion, they undergo detachment-induced cell death, known as anoikis. Anoikis, a unique phenomenon of apoptosis consequential to insufficient cell-matrix interactions (3) is recognized as a significant player in tumor angiogenesis and metastasis (4). During metastatic progression, cells are in a dynamic state, lacking firm attachment to ECM and susceptible to anoikis (4). Thus, resistance to die via anoikis dictates tumor cell survival and provides a molecular basis for therapeutic targeting of metastatic prostate cancer.

Talin1 is a focal adhesion protein that binds to multiple adhesion molecules, including integrins, vinlulin, focal adhesion kinase (FAK), and actin. In addition to structural role, talin1 play an essential role in integrin activation (5). Upon activation, integrins increase the functional interactions between a cell and ECM, thus serving as bidirectional transducers of extracellular and intracellular signals and ultimately regulating adhesion, proliferation, anoikis, survival, and tumor progression (1, 5–7). Therefore, talin1-mediated linkage of integrins to the actin cytoskeleton in focal adhesion complexes is a dynamic, multicomponent plasma membrane–associated assemblies essential for cell adhesion and motility (8). Talin1-deficient mice exhibit failure of integrins to aggregate into clusters and connect to the cytoskeleton, resembling the integrin deficient phenotype and supporting that integrin function is talin1 dependent (9). Recent evidence documents that talin1 suppresses expression of E-cadherin, a cell-cell adhesion effector that negatively correlates with cancer progression, independent of integrin (10), indicating a role for talin1 distinct from the integrin-dependent mechanism. However, the precise role of talin1 in cancer development and progression has not been elucidated.

Authors' Affiliations: [1]Department of Surgery/Urology, University of Kentucky College of Medicine; [2]Mercer University School of Medicine, Division of Basic Medical Sciences, Macon, Georgia; [3]Department of Pathology, University of Pittsburgh Medical Center, Pittsburgh, Pennsylvania; and [4]Department of Molecular and Cellular Biochemistry and [5]Markey Cancer Center, University of Kentucky College of Medicine, Lexington, Kentucky

Note: Supplementary data for this article are available at Cancer Research Online (http://cancerres.aacrjournals.org/).

Corresponding Author: Natasha Kyprianou, University of Kentucky Medical Center, Division of Urology, 800 Rose Street, MS-283, Lexington, KY 40536. Phone: 859-323-9812; Fax: 859-323-1944; E-mail: nkypr2@uky.edu.

doi: 10.1158/0008-5472.CAN-09-2833

Published OnlineFirst February 28, 2010; DOI: 10.1158/0008-5472.CAN-09-2833

The present study investigated the role of talin1 in prostate cancer progression to metastasis. We show that talin1 engages in focal adhesion interactions with the AKT signaling as the intracellular survival mechanism to confer anoikis resistance and promote prostate cancer cell invasion. Talin1 profiling in human prostate cancer specimens revealed a significantly increased talin1 expression in metastases compared with benign and primary prostate tumors.

Materials and Methods

Cell culture and transfections. Human prostate cancer cell lines PC-3, DU-145, LNCaP, and CWR-22, were obtained from the American Type Culture Collection and cultured in RPMI 1640 (Invitrogen) containing 10% fetal bovine serum (Invitrogen) and antibiotics (PenicilinG/Streptomycin, 50 μg/mL). Human vascular endothelial cells and human brain microvascular endothelial cells (HBMEC) were cultured in endothelial basal medium (EGM-2; Cambrex). Transfection was performed using Lipofectamin 2000 reagent (Invitrogen) according to the manufacturer's protocol. PC-3 cells were transfected with pEGFP or green fluorescent protein (GFP)–talin1 plasmids and cloned under G418 selection (Geneticin, Life Technologies Bethesda Research Laboratories). For silencing talin1 expression in prostate cancer cells, the ShRNA talin1 vector (GIPZ ShRNAmir talin1) was obtained from Open Biosystems. After transfection ShRNA talin1 DU-145 cells were selected using puromycin (a resistance marker). Polyclonal populations were pooled under antibiotic selection media, and after several passages, stable cell lines were characterized for each group by Western blotting.

Attachment assay. Cells were seeded in six-well plates (5×10^4 cells per well) coated with fibronectin (BD Biosciences Discovery Labware). After a 10-min attachment period, attached cells were fixed with methanol (100%) and stored at 4°C in PBS for image analysis. Cells were counted in 3×100 fields per well.

Migration assay. Cell cultures (at 75% confluency) were subjected to wounding as previously described (11). At 24 and 48 h postwounding cells migrating to the wounded areas were counted under the microscope.

Transendothelial migration assay. Sterile (12-mm diameter) glass coverslips were coated with Matrigel (Becton Dickson). Coverslips were then seeded (at a density of 6.25×10^4 HBMEC) to form a complete monolayer. Cells were allowed to adhere/spread on the Matrigel for 24 h before initiation of the migration assay. PC-3 and DU-145 cells were resuspended in EGM-2MV (Cambrex) and added to the HBMEC monolayer (8×10^3 cells per coverslip) for 12 h. Cells were subsequently fixed in paraformaldehyde (2% in PBS; 10 min at room temperature) and washed with PBS. Nuclei were stained with 4′,6-diamidino-2-phenylindole (DAPI) nucleic acid stain (Molecular Probes). Slides were visualized and examined under confocal microscopy.

Western blot analysis. Protein expression was determined by immunoblotting using the following specific antibodies. The human polyclonal rabbit talin1 antibody was generated by Dr. Richard McCann. The antibodies against FAK, AKT, phosphorylated Akt (Ser^{473}), p44/42 mitogen-activated protein kinase (MAPK), phosphorylated p42/44 MAPK, glycogen synthase kinase 3β (GSK3β), phosphorylated GSK3β, SRC, and phosphorylated SRC (Tyr^{416}) were obtained from Cell Signaling Technology; phosphorylated FAK (Y^{397}) was obtained from Sigma. Protein levels were normalized to α-actin expression and were detected by using the α-actin antibody from Oncogene Research Products. Cell lysates were prepared using radioimmunoprecipitation assay (RIPA) buffer [150 mmol/L NaCl, 50 mmol/L Tris (pH 8.0), 0.5% deoxycholic acid, 1% NP40 with 1 mmol/L phenyl methyl-sulfonyl fluoride]. Protein content was quantified using the bicinchoninic acid protein assay kit (PierceL), and protein samples (30 μg) were subjected to SDS-PAGE and transferred to Hybond-C membranes (Amersham Pharmacia Biotech). Membranes were blocked in 5% milk in TBS-T (TBS containing 0.05% Tween 20; 1 h at room temperature), and following incubation with the respective primary antibody (overnight at 4°C), membranes were exposed to species-specific horseradish peroxidase–labeled secondary antibodies. Signal detection was achieved with SuperSignal West Dura Extended Duration Substrate (Pierce) and visualized using a UVP Imaging System. Fold change in specific protein expression was determined on the basis of α-actin expression as a loading control.

Immunoprecipitation. DU-145 cells, ShVector control, and Shtalin1 transfectants were lysed in RIPA buffer. Total protein concentration was quantified (as described above), and protein samples (100 μg) were incubated overnight at 4°C with the specific antibody. Controls for the immunoprecipitations were set up by using control IgG derived from the same species as the primary antibody + Protein G/A (second antibody). After incubation of lysates with Protein G Plus/Protein A agarose beads (30 μL) for 3 h at 4°C, beads were washed in PBS buffer, subjected to SDS-PAGE analysis, and transferred to nitrocellulose membranes (Amersham Pharmacia).

AKT inhibitor. The AKT inhibitor 1L6-hydroxymethyl-chiro-inositol-2-(R)-2-*O*-methyl-3-*O*-octadecyl-sn-glycerocarbonate was obtained from Calbiochem; it was used at concentration of 10 μmol/L as previously reported (12).

Apoptosis evaluation. Cells were harvested in EDTA buffer (0.5 mmol/L) and incubated in HBSS supplemented with 2% bovine serum albumin and 0.01% sodium azide (30 min at 4°C). Cells were subsequently fixed in 4% (w/v) formaldehyde in PBS and exposed to Annexin V (R&D Systems) followed by FITC-conjugated secondary antibody. Analysis of Annexin V fluorescence was performed using flow cytometry (Partec).

Caspase-3 activity assay. GFP talin1 and vector control cells were plated on either collagen or nonadhesive polyhydroxyethylmethacrylate (poly-HEMA) and incubated for 6 to 24 h. Caspase-3 activation was measured by Caspase-Glo 3/7 Assay (Promega) according to manufacturer's protocol. Exposure to TNF-related apoptosis-inducing ligand (TRAIL; 100 ng) + Velcade (100 nmol/L) for 16 h was used as a positive control.

Cell cycle arrest evaluation. Cells were fixed with 70% ethanol (30 min at 4°C), stained with propidium iodide (50 μg/mL) containing 20 μg/mL of RNase (30 min at room temperature), and were subsequently subjected to flow cytometric analysis. Cell cycle progression was analyzed via fluorescence-activated cell sorting using the Partec Flow Max.

Anoikis evaluation. Cells were plated on fibronectin or the nonadhesive poly-HEMA–coated dishes and incubated

Published OnlineFirst February 28, 2010; DOI: 10.1158/0008-5472.CAN-09-2833

for 24 h. Cells undergoing apoptosis were detected using the Annexin V immunofluorescence approach and flow cytometric analysis (Partec). Western blotting was used to determine expression of apoptosis regulators after talin1 overexpression/silencing in prostate cancer cells.

Caspase-3 activity assay. GFP talin1 and vector control cells were plated on either collagen or nonadhesive poly-HEMA and incubated for 6 to 24 h. Caspase-3 activation was measured by Caspase-Glo 3/7 Assay (Promega) according to manufacturer's protocol. Exposure to TRAIL (100 ng) + Velcade (100 nmol/L) for 16 h was used as a positive control.

In vivo *experimental metastasis assay.* Human prostate cancer cells were injected (2×10^6/80 μl of PBS) in the tail vein of male nude mice (4–6 wk). After 4 wk mice were sacrificed and the lungs and liver were surgically excised and examined for metastatic lesions under a dissecting microscope (40×).

Transgenic adenocarcinoma mouse prostate transgenic mouse model. The transgenic adenocarcinoma mouse prostate (TRAMP) mice (C57BL/6J) are transgenic mice that express SV40T/t antigens under the prostate-specific rat probasin promoter (13, 14). TRAMP transgenic males develop prostate adenocarcinoma in a manner resembling the clinical progression of human prostate cancer from intraepithelial neoplasia to androgen-independent metastatic tumors. H&E-stained sections of prostate tissues from TRAMP/+/+ male mice were evaluated by two independent investigators (S.S. and N.K.) to confirm pathologic grade. Wild-type (WT) male mice (C57BL/6) of comparable age groups (6–29 wk) served as controls. The histopathologic grading of prostatic tumors was conducted using a standard grading scale in TRAMP mice. Flat lesions and focal cell piling (grade 2.0–2.2) were observed in the majority of 12-wk-old TRAMP mice (Table 1). In 20- to 27-wk-old TRAMP mice, prostates exhibited focal cribriform lesions protruding into the lumen (grades 3–5), representing tumor progression to advanced disease.

Prostate sections from WT and the TRAMP tumors of increasing grade and metastatic lesions (5 μm) were subjected to immunohistochemical analysis for talin1 expression using the talin1 polyclonal antibody (provided by Dr. McCann). Slides were examined under a Nikon fluorescence microscope (Nikon, Inc.). Values were determined in a semiquantitative fashion, incorporating both the intensity of staining and the number of positively stained epithelial cells (15). Briefly, the staining intensity (I) was graded as 0 (absent), 1 (weak), 2 (moderate), or 3 (strong). The proportion (P) of positive epithelial cells (0.0–1.0) with the staining intensity was recorded. A score for each histologic grade (H) was determined as the product of intensity and proportion ($H = I \times P$).

Human prostate specimens. Human prostate tissue specimens from patients with primary and metastatic prostate tumors (Department of Pathology, University of Pittsburgh) were subjected to immunoprofiling for talin1 expression. Computer image analysis determined talin1 expression levels in prostate specimens: 74 normal prostate, 93 normal areas surrounding malignant tissue, 71 benign prostate hyperplasia (BPH) areas, 35 prostate primary tumors (Gleason score, 6–9), and 44 metastatic lesions.

Table 1. Expression of talin1 in human prostate cancer

A. Quantitative analysis of talin1 expression in human prostate tissue

Specimen	(*n*)	Intensity	*P*	
Normal	(42)	155.4 ± 5.3		
Adjacent	(101)	150.2 ± 0.3	0.017*	
BPH	(56)	155.2 ± 6.3	0.319	
Primary tumor	(34)	162.2 ± 7.8	0.00028**	0.0030**
Metastasis	(74)	167.3 ± 7.9	0.0000009**	

B. Talin1 expression in primary prostate tumor

Tumor grade	(*n*)	Intensity	*P*
Gleason 6/7	(15)	154.2 ± 8.7	
Gleason 8	(9)	163.0 ± 10.3	0.0327*
Gleason 9	(10)	167.1 ± 4.5	0.0005**
Gleason 8/9	(19)	164.9 ± 8.2	0.0009**

NOTE: A, talin1 protein expression was evaluated by computer-based imaging. Specimens included normal prostate, normal tissue adjacent to tumor foci, benign prostate hyperplasia, BPH, primary prostate tumor, and lymph node metastasis. * and ** indicate statistical difference at $P < 0.05$ and $P < 0.01$, respectively, compared with normal prostate. B, comparative evaluation of talin1 levels in human primary prostate cancer specimens (Gleason score, 6/7) and poorly differentiated tumors (Gleason score, >8, 8, 9, 8/9). * and ** indicate statistical differences at $P < 0.05$ and $P < 0.01$, respectively, compared with moderately differentiated tumors (Gleason score, 6/7).

Statistical analysis. One-way ANOVA was performed using the StatView statistical program to determine the statistical significance between values ($P < 0.05$). Tissue immunoreactivity was analyzed and interpreted according to previously published protocols (16).

Results

Role of talin1 in prostate tumorigenesis. The expression profile of talin1 was assessed during *in vivo* prostate tumorigenesis in the TRAMP model. As shown in Fig. 1A, talin1 immunoreactivity was primarily detected among the glandular epithelial cells in the TRAMP prostates. Talin1 protein levels progressively increased with increasing age of TRAMP mice (6–27 weeks) (Fig. 1A, iii–vi). There was weak talin1 immunoreactivity in prostate tissue from WT control mice, whereas the intensity of talin1 staining was considerably stronger in primary prostate tumors, with the highest detected in liver metastases (Fig. 1A, ii). Quantitative analysis revealed a 2-fold increase in talin1 levels in prostate tumors derived from the 12-week-old TRAMP mice compared with the 6-week-old TRAMP mice (Fig. 1B). By 27 weeks of age, at which time TRAMP mice exhibit a highly aggressive prostate tumor

Published OnlineFirst February 28, 2010; DOI: 10.1158/0008-5472.CAN-09-2833

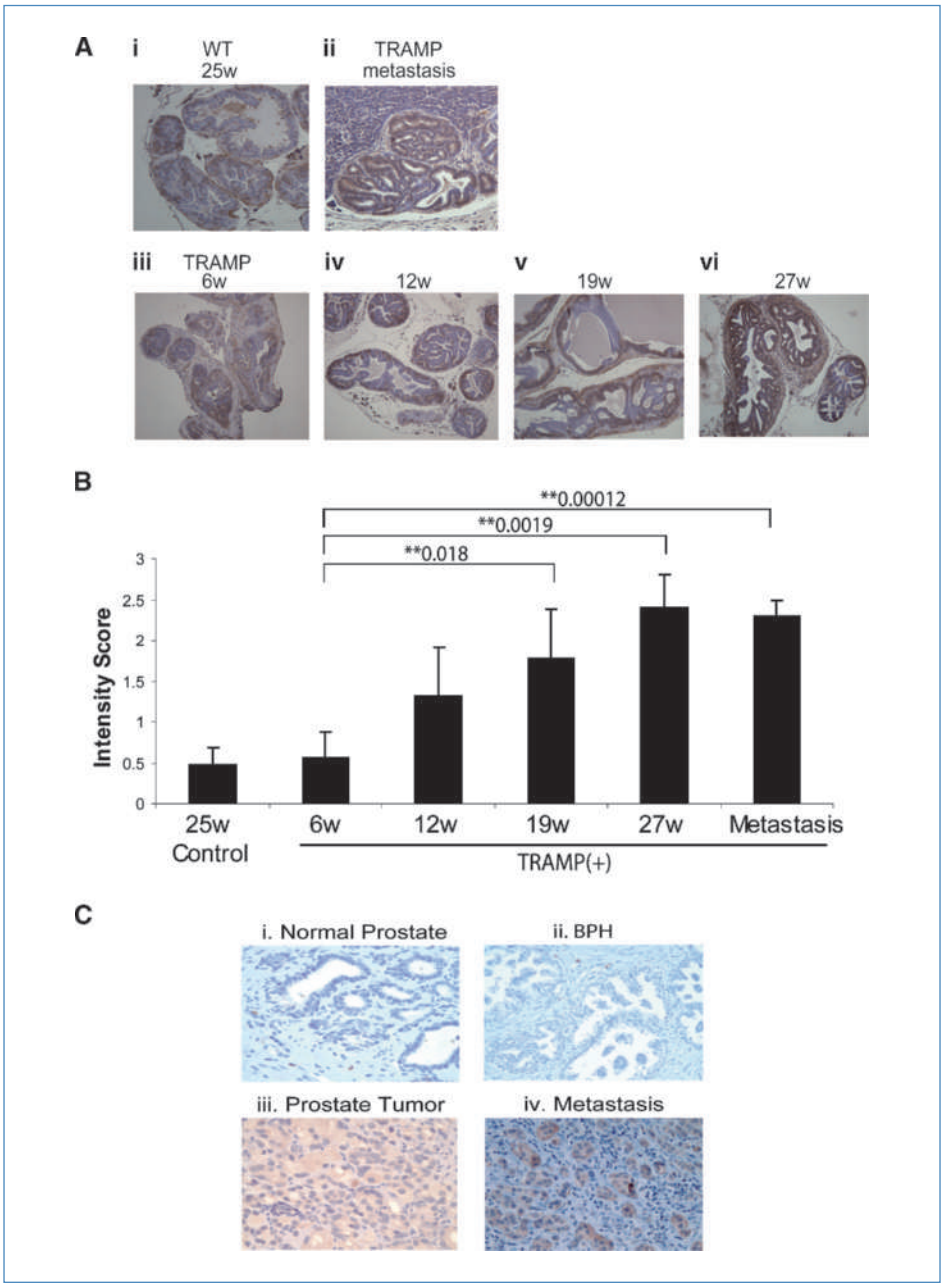

Figure 1. Talin1 profiling during prostate tumor progression in the TRAMP model and human prostate cancer specimens. A, talin1 expression was analyzed in paraffin-embedded prostate tissue specimens from TRAMP mice and control age-matched mice (6–27 wk). A strong immunoreactivity for talin1 was detected in prostate tumors derived from both 19- and 27-wk-old TRAMP mice (iv and v, respectively). ii, a metastatic lesion to the liver in a TRAMP mouse (27 wk). B, the intensity of immunohistochemical staining (*H*) was calculated by *P* = percentage of staining × *I* intensity (1–3). The numerical data reveal a positive correlation between increasing tumor grade and progression to metastasis and increased talin1 expression. * and ** indicate statistical difference at $P < 0.05$ and $P < 0.01$, respectively, compared with specimens from control mice. C, talin1 immunoreactivity was analyzed in paraffin-embedded prostate tissue specimens from normal (i), BPH (ii), primary prostate tumors (iii), and metastasis (iv).

phenotype (grades 4.5–5), talin1 expression increased significantly ($P = 0.0019$; Fig. 1B).

Talin1 correlates with human prostate cancer progression. To determine significance of talin1 in human prostate cancer progression to metastatic disease, we conducted immunohistochemical staining for talin1 in human prostate tissue specimens (Fig. 1C). Talin1 expression was analyzed in 307 human prostate tissue specimens, including 74 normal, 101 adjacent areas to the tumor, 56 BPH, 34 primary tumors (Gleason score, 6–9), and 74 metastatic lesions (Table 1A). Immunoreactivity was quantitated by automated quantitative analysis to determine the cytoplasmic levels of talin1. A representative picture of normal prostate, BPH, primary prostate tumor, and metastatic lesion to the lymph node is shown in Fig. 1C (i–iv). Cytoplasmic talin1 expression was significantly higher in primary tumor and metastasis lesion compared with normal prostate ($P < 0.00028$, $P < 0.0001$, respectively), whereas talin1 expression detected in BPH specimens was comparable with those detected in normal prostate tissue ($P = 0.319$). Talin1 expression in metastatic lesions was significantly higher compared with primary tumors ($P < 0.0001$; Table 1A). The intensity of talin1 immunoreactivity in poorly differentiated prostate tumors (Gleason score, 8/9) was significantly higher compared with

Published OnlineFirst February 28, 2010; DOI: 10.1158/0008-5472.CAN-09-2833

moderately differentiated tumors (Gleason score, 6/7; P = 0.0009). Talin1 levels also increased with increasing Gleason score (Gleason score, 6/7–9; Table 1B).

Talin1 promotes prostate cancer cell adhesion, migration, and invasion. The effect of talin1 overexpression on the adhesion ability and migration potential of prostate cancer cells were examined *in vitro*. The endogenous expression of talin1 was profiled in human prostate cell lines as well as prostate fibroblasts (as positive control for talin1 abundance). DU-145 prostate cancer cells exhibited the highest talin1 expression (Fig. 2A). GFP talin1 stable transfectants were generated in PC-3 cells, which express very low endogenous talin1 levels (Fig. 2A). Overexpression of talin1 (Fig. 2A, right) significantly increased both the adhesion (Fig. 2B) and migration potential of prostate cancer cells (Fig. 2C) compared with vector control cells. To determine the consequences of talin1 overexpression on the invasive potential of prostate cancer cells through an endothelial cell monolayer, transendothelial migration (TEM) assay was performed using HBMECs. As shown on Fig. 2D, talin1 overexpression led to a significant increase in prostate cancer cell invasion through the endothelial cell monolayer ($P < 0.01$).

Prostate tumor epithelial cell survival requires continuous attachment to the ECM, and it is recognized that fibronectin, laminin, and collagen participate in the formation of attachment plagues linked to the actin cytoskeleton. The effect of talin1 loss on prostate cancer cell adhesion was examined by generating ShRNA talin1 stable transfectants in DU-145 prostate cancer cells that are characterized by high endogenous talin1 expression (Fig. 3A). As shown on Fig. 3A, ShRNA silencing of talin1 effectively reduced talin1 expression in DU-145 cells (>80%). Talin1-silenced DU-145 cells exhibited a reduced ability to adhere to different ECM components, including collagen, laminin, and fibronectin (Fig. 3B). Furthermore loss of talin1 led to significant reduction in the migration potential compared with vector control cells (Fig. 3C). Examination of the invasion ability of talin1-silenced transfectants through an endothelial cell monolayer revealed a significant suppression (Fig. 3D).

Talin1 facilitates ECM-integrin–mediated focal adhesion signals. The mechanism via which talin1 activates intracellular signals was investigated in the context of ECM–epithelial cell interaction. We focused on FAK/AKT signaling and intracellular MAPK pathway, as both have been implicated in

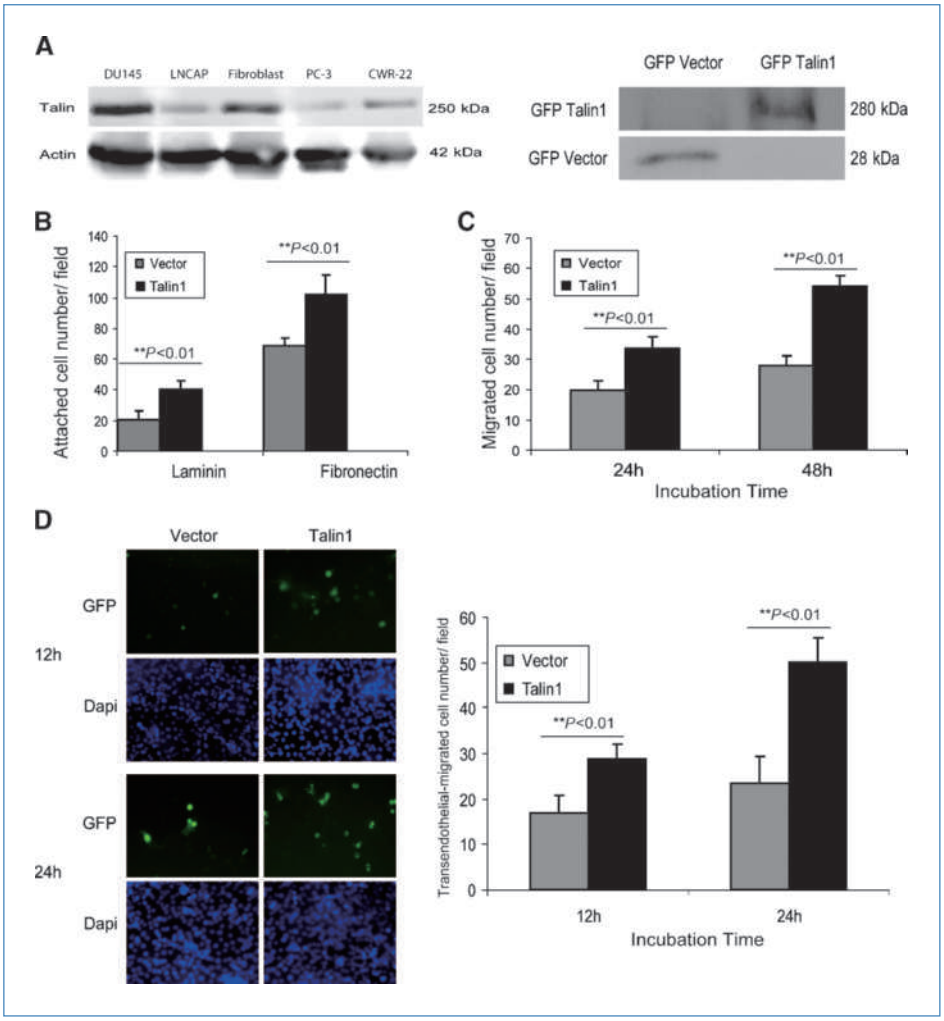

Figure 2. Talin1 enhances cell adhesion, migration, and invasion. A, talin1 endogenous expression in human prostate cancer cell lines; actin expression is used as a loading control. Bands detected indicate GFP talin1 (280 kDa) and GFP vector protein (28 kDa). B, cell adhesion potential was comparatively analyzed in laminin- or fibronectin-coated plates in PC-3 GFP vector control and PC-3 GFP talin1 cloned transfectants. Values represent the mean from three independent experiments performed in duplicate ± SEM. C, PC-3 cells were subjected to wounding, and migrating cells were counted under the microscope in three independent fields (three wells per condition). D, TEM assay was performed using HBMECs and either PC-3 GFP vector or PC-3 GFP talin1 expressing cells, as described in Materials and Methods. Green and blue staining indicated GFP vector/talin1 cells and DAPI nuclear staining, respectively. Numerical data (right) represent values from three independent experiments ± SEM.

Published OnlineFirst February 28, 2010; DOI: 10.1158/0008-5472.CAN-09-2833

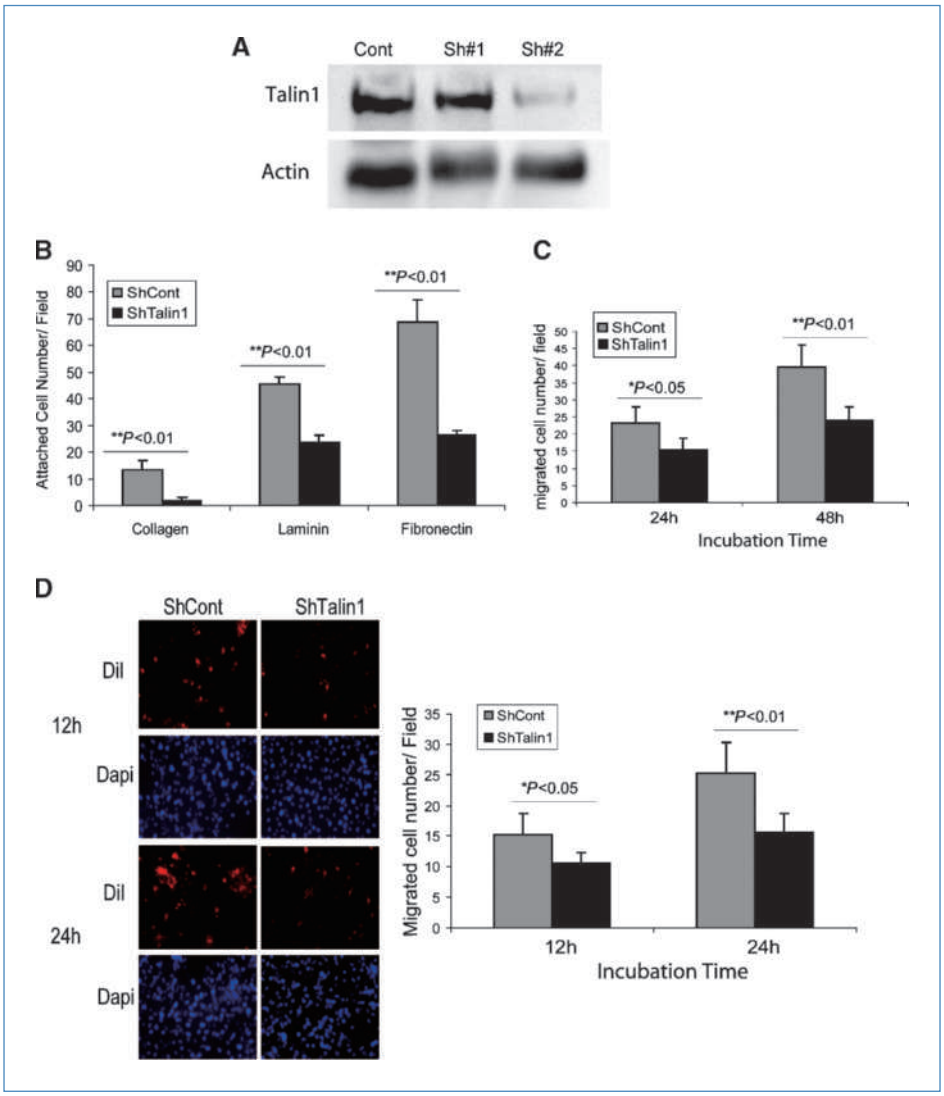

Figure 3. Talin1 loss decreases cell adhesion, migration, and invasion. A, ShRNA talin1 stable cell line was established in DU-145 cells. B, ShRNA vector and ShRNA talin1 transfectant cells were comparatively analyzed for their adhesion potential (as described above). Values represent mean ± SEM from three independent experiments. C, Talin1 silencing reduces DU-145 cell migration ability. Cells were subjected to wounding, and their migration potential was evaluated; the number of migrating cells was counted under the microscope in three independent fields (40×) per well (three wells per condition). D, loss of talin1 inhibits prostate tumor cell invasion. TEM assay was conducted using HBMEC DU-145 vector and ShRNA talin1 stable cell line. The number of invading cells (red) was determined under confocal microscopy after 12 and 24 h. Blue color represents DAPI nuclear staining.

integrin-focal adhesion-dependent signals (17). Activation of FAK due to phosphorylation (Y^{397}) was observed on collagen attachment conditions, whereas it was more prominent on fibronectin-coated ECM in talin1-overexpressing cells relative to control cells (Fig. 4A). Talin1 overexpression in prostate cancer cells (PC-3) also resulted in a marked activation on phosphorylation of AKT (Ser^{473}) under fibronectin attachment conditions, whereas only a modest activation of p44/42 MAPK was observed (Fig. 4A). These observations were confirmed by fluorescence microscopy (data not shown). There was a significant enhancement in the phosphorylation of FAK, AKT, and MAPK when cells were cultured on fibronectin-coated surface (Fig. 4B). Talin1 overexpression induced AKT phosphorylation as early as 3 hours after adhesion, with continuous activation after 24 hours (Fig. 4B, right).

The effect of talin1 on integrin–focal adhesion complex signaling interactions was subsequently investigated by examining the direct binding of talin1 to integrin β3, a key talin1

Figure 4. Talin1 mediates ECM-dependent activation of FAK/AKT pathway. A, after adherence of GFP talin1 and vector-transfected PC-3 cells on either collagen or fibronectin plates (6 h), cells were lysed and subjected to Western blot analysis. Levels of total and phosphorylated AKT (Ser^{473}), FAK (Y^{397}), and MAPK proteins were detected using respective antibodies. B, phosphorylation of AKT (Ser^{473}), FAK (Y^{397}), and MAPK were evaluated after (6 h) adherence to fibronectin. Quantification of phosphorylation was performed by densitometry (right). C, ShTalin1 DU-145 cells were subjected to immunoprecipitation using the integrin β3 antibody or the ILK-1 antibody. As controls, proteins were precipitated with the control IgG derived from the same species plus the secondary antibody (protein G/A). Talin1, total FAK, and SRC binding were detected by Western blotting. Binding of ILK-1 or integrin β3 was determined using the respective antibodies (right). D, GFP vector and talin1-expressing PC-3 cells were plated on fibronectin-coated plate incubated with mouse IgG or integrin β3 (blocking) antibodies (20 μg/mL). The total proteins and phosphorylated forms of FAK and AKT were determined by immunblotting after 6 h of plating.

Published OnlineFirst February 28, 2010; DOI: 10.1158/0008-5472.CAN-09-2833

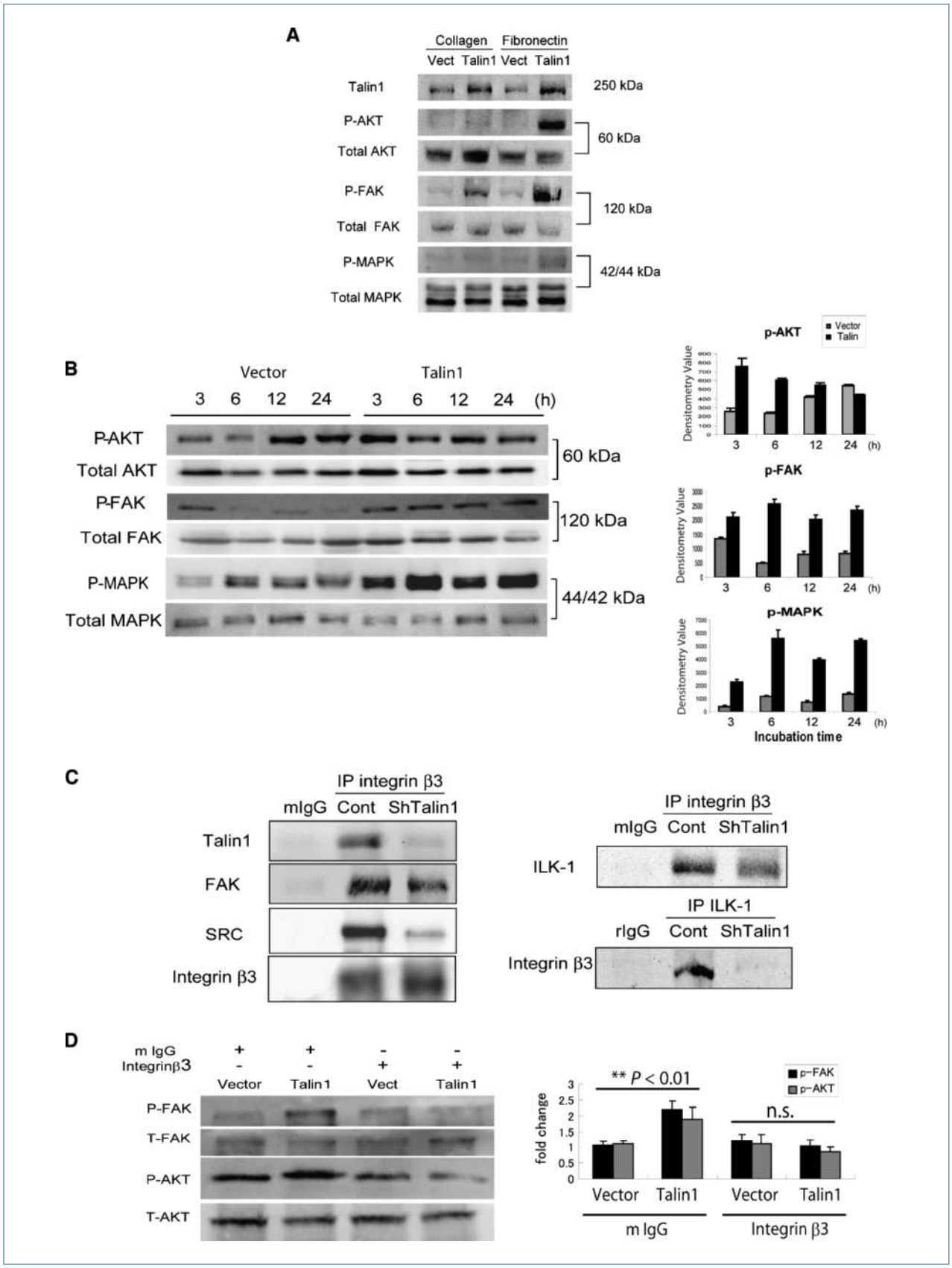

Published OnlineFirst February 28, 2010; DOI: 10.1158/0008-5472.CAN-09-2833

binding partner (18). To this end we used the DU-145 cell line, which exhibits high endogenous expression of integrin β3 (data not shown). Talin1 silencing significantly reduced talin1 binding to integrin β3 as well as the focal adhesion partners, FAK and Src (Fig. 4C). The reduced binding of Src upon talin1 loss (Fig. 4C) led us to probing the role of integrin-linked kinase-1 (ILK-1), a protein that regulates Src binding in response to integrin activation. Immunoprecipitation by integrin β3 revealed a significant decrease in ILK-1 binding in talin1-silenced prostate cancer cells. Immunoprecipitation by ILK-1 revealed that talin1 loss abrogated ILK-1 binding to integrin β3 complex (Fig. 4C, right). In the presence of a blocking antibody against integrin β3, there was a significant reduction in the phosphorylation of AKT and FAK in talin1-overexpressing cells (Fig. 4D).

Talin1 mediates anoikis resistance. To investigate the integrin-independent role for talin1 (10), we examined the effect of talin1 overexpression on cell suspension conditions. Cells were plated on either fibronectin-coated matrix or nonadhesive poly-HEMA. As shown on Fig. 5A, talin1 did not lead to a significant apoptotic effect in adherent conditions, but under nonadherent conditions, talin1-overexpressing cells exhibited a significant reduction in apoptosis as detected by Annexin V staining (Fig. 5A), suppression of caspase-3 activity (Fig. 5B), activation of AKT survival signaling (Fig. 5C), and subpopulation G_0-G_1 arrest (Supplementary Fig. S1). Talin1-overexpressing cells exhibited a moderate activation of FAK (Y^{397}), AKT (Ser^{473}), and Src (nonadherent conditions), although the response was weaker than under fibronectin conditions (Fig. 5C). Analysis of the anchorage-independent phosphorylation of these proteins revealed a significant time-dependent increase in phosphorylation of FAK, AKT, and Src in talin1-overexpressing cells, which was paralleled by a reduction in caspase-3 activation (Fig. 5C, right). Considering the evidence that ILK-1 is an effective signaling mediator of anoikis resistance (19), we also examined GSK3β activation, a direct target for ILK-1, under nonadherent conditions. Talin1-overexpressing cells exhibited increased phosphorylation of GSK3β and reduced caspase-3 cleavage compared with vector control cells, indicating anokis suppression (Fig. 5C, right). Resistance to anoikis is recognized as a critical mechanism underlying tumor cell metastatic dissemination (4). Thus subsequent studies pursued the functional characterization of talin1 in determining the metastatic potential of prostate cancer cells *in vivo*. Talin1 loss in prostate cancer cells led to a significantly reduced number of metastatic tumor lesions (to the lungs; Fig. 5D).

AKT involvement in talin1 mediated migration and invasion but not adhesion. To determine whether AKT activation is an integral part of talin1 intracellular signaling, the consequences of AKT inhibition on talin1-mediated biological effects were examined. As shown on Supplementary Fig. S2, AKT inhibition had no significant effect on the adhesion potential of talin1-overexpressing prostate cancer cells on either fibronectin- or laminin-coated matrix. In the presence of the AKT inhibitor, both the migration potential and invasion ability of talin1-overexpressing cells (Supplementary Fig. S2) were significantly suppressed compared with the vector control cells ($P < 0.01$).

Discussion

Tumor cells develop mechanisms to resist anoikis, which enables their survival after detachment from the primary site and travel through the lymphatic and circulatory systems to distant organs (4). The present study identifies talin1 as a novel regulator of prostate cancer cell invasion and metastatic potential via its survival signaling by activating the ECM-integrin–mediated signaling and promoting anoikis resistance. Talin1 overexpression significantly enhanced the migration and invasion potential of human prostate cancer cells in an AKT-dependent manner. In contrast, loss of talin1 led to a diminished invasion potential and *in vivo* metastatic ability of prostate cancer cells. These results are in accord with a previous screening reporting that highly metastatic cells expressed significantly high levels of talin1 (>16-fold, second highest of 440 proteins screened) compared with less metastatic cells (20). Interestingly enough, talin1 mRNA has been shown to be downregulated by androgens in primary prostate cancer cells (21). Our *in vivo* findings in the TRAMP model of prostate tumorigenesis reveal a positive correlation between talin1 immunoreactivity and prostate cancer progression to metastasis. A dramatic increase in talin1 expression was detected in prostate tumors from 12-week-old TRAMP mice, and talin1 levels were further increased with tumor progression to advanced metastatic disease. Taken together, these lines of evidence support an indirect link between talin1 and prostate cancer metastasis and emergence to androgen independence.

Overexpressing talin1 in prostate cancer cells led to activation of FAK/AKT signaling via both an ECM-dependent and -independent mechanism. Gaining support from evidence that AKT survival signaling is causally linked to anoikis resistance in detached cells (22, 23), our data indicate that talin1 promotes tumor cells to metastasize by enhancing their local invasive properties and survival after detachment from the primary tumor site via activation of FAK and AKT signaling. This resonates with a similar role assigned to another key focal adhesion protein, paxillin, in different tumors. Indeed, overexpression of paxillin correlates with metastatic and invasion properties in hepatocellular carcinoma (24). Recruitment of FAK and paxillin to β1 integrin promotes cancer cell migration through MAPK activation (25). The present findings suggest that talin1 might not be causally involved in primary tumor development and growth but rather in promoting local invasion, as well as distant metastasis, via targeting the ECM-integrin–mediated signaling and resistance to anoikis.

Resistance to anoikis, potentially conferred by talin1, is not a selective advantage during tumor growth in an ECM-rich microenvironment, rather during the invasion through vasculature during metastasis. Resistance to anoikis could predict a greater ability to form metastatic lesions. The idea resonates with the evidence gathered from the analysis of human prostate cancer specimens. The highest talin1 protein expression was found in metastatic lesions compared with benign areas and primary prostate tumor sites (Table 1A). Interestingly enough there was a gradient of increasing expression within the primary tumors of increasing Gleason score (Table 1B).

Published OnlineFirst February 28, 2010; DOI: 10.1158/0008-5472.CAN-09-2833

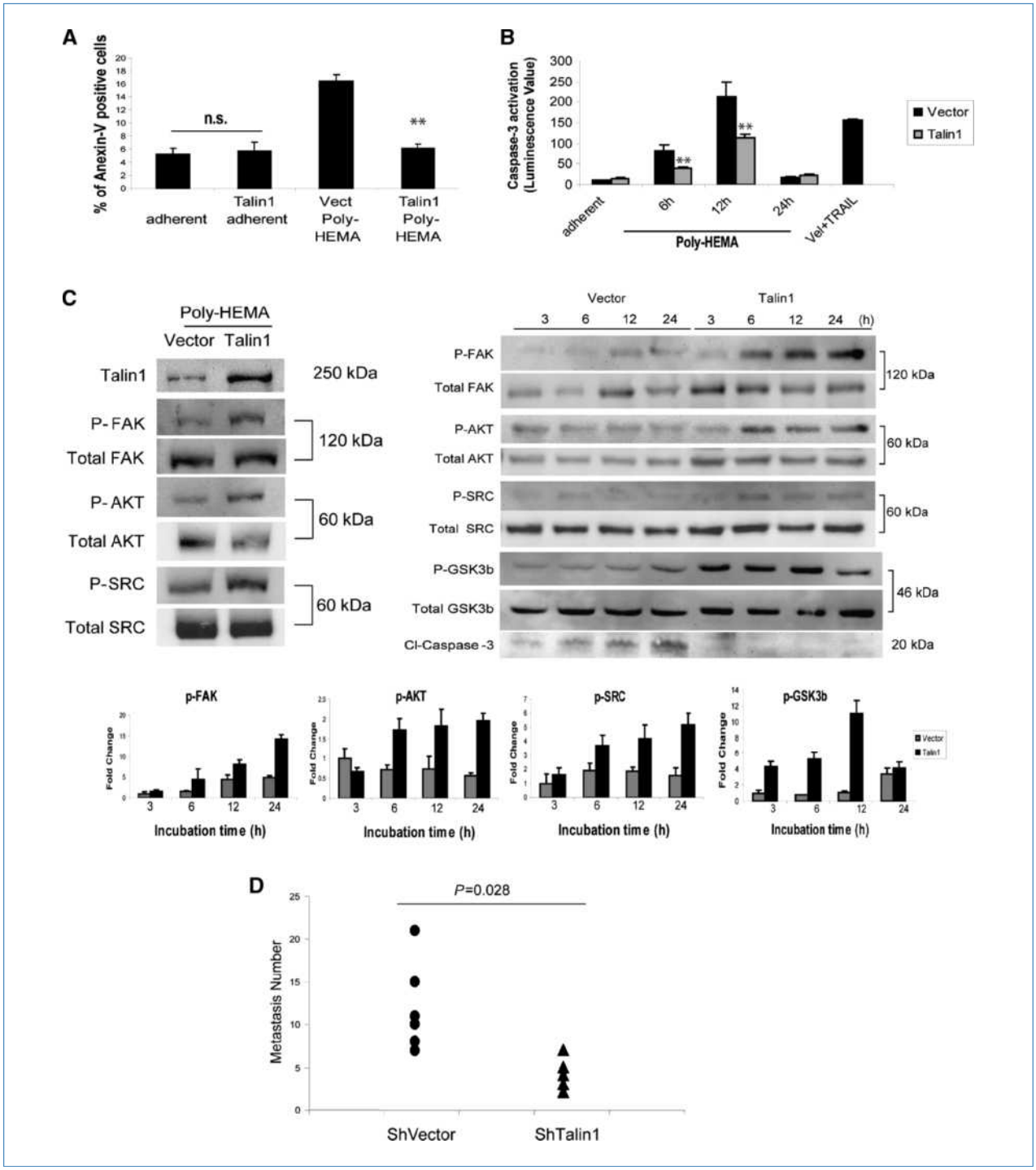

Figure 5. Talin1 mediates anoikis resistance. A, GFP talin1 and vector PC-3 cells were kept in suspension conditions using poly-HEMA–coated plates for 24 h and subjected to flow cytometry using AnnexinV antibody. B, caspase-3 activation was measured in poly-HEMA suspension conditions after 6, 12, and 24 h, as described in Materials and Methods. GFP talin1 and GFP vector cells were also treated with TRAIL (100 ng/mL) plus Velcade (100 nmol/L; positive control). Values indicate the mean from two independent experiments performed in triplicate ± SEM. **, statistically significant difference at $P < 0.01$. C, GFP talin1 and vector PC-3 cells were kept in suspension conditions, and after 24 h, cells were lysed and subjected to Western blotting. Expressions of total protein and phosphorylated forms of AKT (Ser^{473}), FAK (Y^{397}), and p42/44 MAPK were detected using respective antibodies (left). Levels of total and phosphorylated AKT (Ser^{473}), FAK (Y^{397}), SRC, and GSK3β, as well as cleaved caspase-3, were assessed during different time points (3–24 h; right). The phosphorylation status of individual proteins was evaluated by densitometry (bottom). D, experimental metastasis assay. Nude mice were injected i.v. in the tail vein with prostate cancer cells: DU-145 ShVector ($n = 6$) and DU-145 ShRNA talin1 [$n = 5$ (2×10^6 per mouse)]. At 5 wk postinoculation, lungs were dissected and metastastic lesions were counted. Talin1 loss led to a significantly reduced number of metastatic lesions to the lungs ($P = 0.028$).

Published OnlineFirst February 28, 2010; DOI: 10.1158/0008-5472.CAN-09-2833

This points to a promising value of talin1 expression in primary tumors as a predictor of metastatic potential, because prostate tumors with high Gleason score (>8) are pathologically recognized as high-risk adenocarcinoma and those patients have limitations in treatment options due to higher incidence of distant metastasis that significantly limits prognosis (26). A similar functional contribution in enhancing metastasis, but not primary tumor growth, was shown by the apoptotic suppressor of cytoskeleton-dependent death Bcl-Xl during mammary carcinogenesis (27).

Mechanistic dissection revealed that talin1 promotes ILK-1 binding to integrin β3 subunit; this evidence implicates ILK-1, as an intracellular effector of talin1 signaling, activated upstream of the AKT survival pathway. ILK is a serine/threonine protein kinase that interacts with cytoplasmic domain of β1-integrin and β3-integrin and has been functionally linked to integrin and Wnt signaling pathways (28–30). ILK regulates several integrin-mediated cellular processes, including cell adhesion, fibronectin-ECM assembly, and anchorage-dependent cell growth (29, 31, 32). Upon cell adhesion, ILK is transiently activated and directly phosphorylates AKT Ser^{473} (33) and GSK3 (31). In contrast, inhibiting ILK in cancer cells inhibits AKT phosphorylation and cell survival. ILK-1 mediates anoikis resistance even without activation of integrin/ECM signals, possibly via recruiting through α-parvin–mediated targeting of AKT to lipid rafts (19, 34, 35). Our *in vitro* data suggest that talin1 facilitates direct ECM–epithelial cell interaction and confers anoikis resistance.

Based on these findings we propose that talin1 is responsible for the acquisition of the primary prostate tumor cell invasive and metastatic properties leading to metastasis. In the schematic scenario shown on Supplementary Fig. S3, under adherent conditions, talin1 facilitates integrin signaling and its link to the ECM. Talin1 binding to β integrin recruits the focal adhesion proteins ILK, FAK, and Src toward activation of the downstream signals, such as AKT and extracellular signal-regulated kinase. These signaling events promote cell survival, invasion, and angiogenesis. Under nonadherent conditions, talin1 stimulates FAK, Src, and GSK3β independent of integrin signaling and confers resistance to anoikis, leading to metastatic spread (Supplementary Fig. S3). Our attempts to analyze the direct interaction of talin1 with ILK-1 or β integrin did not provide clear evidence of such interactions under nonadherent conditions. This might be attributed to weak "bonding" interactions relative to the adherent focal adhesion complex by additional proteins responsible for transducing talin1 signaling under nonadherent conditions.

The clinical relevance of our findings relates to the significant increase in talin1 expression in primary tumors and metastatic prostate cancer compared with benign and normal prostate. The metastatic specimens exhibited significantly higher talin1 levels compared with primary prostate tumors, implicating an involvement of talin1 in the metastatic process. These results suggest that talin1 may have diagnostic values in prostate cancer detection and clinical outcome. Ongoing studies focus on a correlation between talin1 expression with serum PSA levels, Gleason grade, and patient (disease-free) survival in a large cohort of prostate cancer patients, which may define the value of talin1 as a cancer metastasis marker. The interaction with other talin1 binding candidates, including paxillin and vinculin, and the effect of such interactions on the phosphorylation status of critical downstream anoikis repression signaling effectors are the focus of ongoing studies. Because talin1 contains multiple phosphorylation sites, including PKA, PKC, and GSK3, as predicted by mass spectrometry (36), it is tempting to propose a potential strategy to target these phosphorylation sites to block talin1-mediated survival signaling in tumor cells. Further dissection of the functional contribution of talin1 in dictating tumor cell and endothelial survival outcomes may provide new opportunities for therapeutic targeting of metastatic prostate cancer.

In summary, the evidence presented supports a regulatory role for talin1 in tumor cell invasion and prostate cancer metastasis via conferring anoikis resistance. Future studies will pursue the generation of a conditional knockout mouse model of talin1, selectively targeting talin1 gene expression in prostate epithelial cells and its crossing with a transgenic mouse model of prostate cancer.

Disclosure of Potential Conflicts of Interest

There are no potential conflicts.

Acknowledgments

We thank Dr. Hong Pu for the animal experiments, Matthew Martelli for the initial contribution to the *in vitro* analysis of talin1, Dr. Barbara Foster (Roswell Park Cancer Institute) for the expert help with the TRAMP mouse model and specimen acquisition, Dr. Steven Schwarze (Department of Biochemistry) and Dr. Chendil Damodaran (College of Health Science) for useful discussions, and Lorie Howard for assistance with the manuscript submission process.

Grant Support

NIH R01 CA107575-06 grant (N. Kyprianou), Markey Cancer Foundation grant (N. Kyprianou), and American Cancer Society IRG grant (R.O. McCann). Shinichi Sakamoto is an American Urological Association Foundation Research Scholar.

The costs of publication of this article were defrayed in part by the payment of page charges. This article must therefore be hereby marked *advertisement* in accordance with 18 U.S.C. Section 1734 solely to indicate this fact.

Received 07/31/2009; revised 11/13/2009; accepted 12/09/2009; published OnlineFirst 02/16/2010.

References

1. Fornaro M, Manes T, Languino LR. Integrins and prostate cancer metastases. Cancer Metastasis Rev 2001;20:321–31.
2. McKenzie S, Kyprianou N. Apoptosis evasion: the role of survival pathways in prostate cancer progression and therapeutic resistance. J Cell Biochem 2006;97:18–32.
3. Frisch SM, Screaton RA. Anoikis mechanisms. Curr Opin Cell Biol 2001;13:555–62.
4. Rennebeck G, Martelli M, Kyprianou N. Anoikis and survival connections in the tumor microenvironment: is there a role in prostate cancer metastasis? Cancer Res 2005;65:11230–5.

Published OnlineFirst February 28, 2010; DOI: 10.1158/0008-5472.CAN-09-2833

5. Giancotti FG, Ruoslahti E. Integrin signaling. Science 1999;285:1028–32.
6. Calderwood DA. Integrin activation. J Cell Sci 2004;117:657–66.
7. Alam N, Goel HL, Zarif MJ, et al. The integrin-growth factor receptor duet. J Cell Physiol 2007;213:649–53.
8. Tanentzapf G, Brown NH. An interaction between integrin and the talin FERM domain mediates integrin activation but not linkage to the cytoskeleton. Nat Cell Biol 2006;8:601–6.
9. Brown NHGS, Rickoll WL, Fessler LI, Prout M, White RA, Fristrom JW. Talin is essential for integrin function in *Drosophila*. Dev Cell 2002;3:569–79.
10. Becam IE, Tanentzapf G, Lepesant JA, Brown NH, Huynh JR. Integrin-independent repression of cadherin transcription by talin during axis formation in *Drosophila*. Nat Cell Biol 2005;7:510–6.
11. Keledjian K, Garrison JB, Kyprianou N. Doxazosin inhibits human vascular endothelial cell adhesion, migration, and invasion. J Cell Biochem 2005;94:374–88.
12. Hu Y, Qiao L, Wang S. 3-(Hydroxymethyl)-bearing phosphatidylinositol ether lipid analogues and carbonate surrogates block PI3-K, Akt, and cancer cell growth. J Med Chem 2000;43:3045–51.
13. Gingrich JRBR, Foster BA, Greenberg NM. Pathologic progression of autochthonous prostate cancer in the TRAMP model. Prostate Cancer Prostatic Dis 1999;2:70–5.
14. Greenberg NMDF, Finegold MJ, Medina D, et al. Prostate cancer in a transgenic mouse. Proc Natl Acad Sci U S A 1995;92:3439–43.
15. Zeng L, Rowland RG, Lele SM, Kyprianou N. Apoptosis incidence and protein expression of p53, TGF-β receptor II, p27Kip1, and Smad4 in benign, premalignant, and malignant human prostate. Hum Pathol 2004;35:290–7.
16. Camp RL, Chung GG, Rimm DL. Automated subcellular localization and quantification of protein expression in tissue microarrays. Nat Med 2002;8:1323–7.
17. Bouchard VDM, Thibodeau S, Laquerre V, et al. Fak/Src signaling in human intestinal epithelial cell survival and anoikis: differentiation state-specific uncoupling with the PI3-K/Akt-1 and MEK/Erk pathways. J Cell Physiol 2007;212:717–28.
18. Calderwood DA, Yan B, de Pereda JM, et al. The phosphotyrosine binding-like domain of talin activates integrins. J Biol Chem 2002;277:21749–58.
19. Hannigan G, Troussard AA, Dedhar S. Integrin-linked kinase: a cancer therapeutic target unique among its ILK. Nat Rev 2005;5:51–63.
20. Everley PAKJ, Zetter BR, Gygi SP. Quantitative cancer proteomics: stable isotope labeling with amino acids in cell culture (SILAC) as a tool for prostate cancer research. Mol Cell Proteomics 2004;3:729–35.
21. Betts AMCG, Neal DE, Robson CN. Paracrine regulation of talin mRNA expression by androgen in human prostate. FEBS Lett 1998;434:66–70.
22. Chang LCHC, Cheng CH, Chen BH, Chen HC. Differential effect of the focal adhesion kinase $Y^{397}F$ mutant on v-Src-stimulated cell invasion and tumor growth. J Biomed Sci 2005;12:571–85.
23. Irie HY, Pearline RV, Grueneberg D, et al. Distinct roles of Akt1 and Akt2 in regulating cell migration and epithelial-mesenchymal transition. J Cell Biol 2005;171:1023–34.
24. Li HGXD, Shen XM, Li HH, Zeng H, Zeng YJ. Clinicopathological significance of expression of paxillin, syndecan-1 and EMMPRIN in hepatocellular carcinoma. World J Gastroenterol 2005;11:1445–51.
25. Crowe DLOA. Recruitment of focal adhesion kinase and paxillin to β1 integrin promotes cancer cell migration via mitogen activated protein kinase activation. BMC Cancer 2004;4:18.
26. Partin AW, Kattan MW, Subong EN, et al. Combination of prostate specific antigen, clinical stage and Gleason score to predict pathological stage of localized prostate cancer. A multi-institutional update. JAMA 1997;277:1445–51.
27. Martin SS, Ridgeway AG, Pinkas J, et al. A cytoskeleton-based functional genetic screen identifies Bcl-xL as an enhancer of metastasis, but not primary tumor growth. Oncogene 2004;23:4641–5.
28. Wu C, Dedhar S. Integrin-linked kinase (ILK) and its interactors: a new paradigm for the coupling of extracellular matrix to actin cytoskeleton and signaling complexes. J Cell Biol 2001;155:505–10.
29. Hannigan GE, Leung-Hagesteijn C, Fitz-Gibbon L, et al. Regulation of cell adhesion and anchorage-dependent growth by a new β1-integrin-linked protein kinase. Nature 1996;379:91–6.
30. Li F, Liu J, Mayne R, Wu C. Identification and characterization of a mouse protein kinase that is highly homologous to human integrin-linked kinase. Biochim Biophys Acta 1997;1358:215–20.
31. Cieslik K, Zembowicz A, Tang JL, Wu KK. Transcriptional regulation of endothelial nitric-oxide synthase by lysophosphatidylcholine. J Biol Chem 1998;273:14885–90.
32. Radeva G, Petrocelli T, Behrend E, et al. Overexpression of the integrin-linked kinase promotes anchorage-independent cell cycle progression. J Biol Chem 1997;272:13937–44.
33. Lynch DK, Ellis CA, Edwards PA, Hiles ID. Integrin-linked kinase regulates phosphorylation of serine 473 of protein kinase B by an indirect mechanism. Oncogene 1999;18:8024–32.
34. Attwell S, Roskelley C, Dedhar S. The integrin-linked kinase (ILK) suppresses anoikis. Oncogene 2000;19:3811–5.
35. Fukuda T, Chen K, Shi X, Wu C. PINCH-1 is an obligate partner of integrin-linked kinase (ILK) functioning in cell shape modulation, motility, and survival. J Biol Chem 2003;278:51324–33.
36. Ratnikov B, Ptak C, Han J, Shabanowitz J, Hunt DF, Ginsberg MH. Talin phosphorylation sites mapped by mass spectrometry. J Cell Sci 2005;118:4921–3.

Cancer Research
The Journal of Cancer Research (1916–1930) | The American Journal of Cancer (1931–1940)

AACR American Association for Cancer Research

Talin1 Promotes Tumor Invasion and Metastasis via Focal Adhesion Signaling and Anoikis Resistance

Shinichi Sakamoto, Richard O. McCann, Rajiv Dhir, et al.

Cancer Res 2010;70:1885-1895. Published OnlineFirst February 28, 2010.